Development of ferroelectric order in relaxor $(1-x)$Pb(Mg$_{1/3}$Nb$_{2/3}$)O$_3$−xPbTiO$_3$ ($0\leqslant x\leqslant 0.15$)

Z.-G. Ye,* Y. Bing, J. Gao, and A. A. Bokov

Department of Chemistry, Simon Fraser University, Burnaby, British Columbia, Canada V5A 1S6

P. Stephens

Department of Physics and Astronomy, State University of New York at Stony Brook, Stony Brook, New York 11794-3800

B. Noheda and G. Shirane

Physics Department, Brookhaven National Laboratory, Upton, New York 11973-500

The microstructure and phase transition in relaxor ferroelectric Pb(Mg$_{1/3}$Nb$_{2/3}$)O$_3$ (PMN) and its solid solution with PbTiO$_3$ (PT), PMN-xPT, remain to be some of the most puzzling issues of solid-state science. In the present work we have investigated the evolution of the phase symmetry in PMN-xPT ceramics as a function of temperature ($20 < T < 500$ K) and composition ($0 \leqslant x \leqslant 0.15$) by means of high-resolution synchrotron x-ray diffraction. Structural analysis based on the experimental data reveals that the substitution of Ti^{4+} for the complex B-site (Mg$_{1/3}$Nb$_{2/3}$)$^{4+}$ ions results in the development of a clean rhombohedral phase at a PT concentration as low as 5%. The results provide insight into the development of ferroelectric order in PMN-PT, which has been discussed in light of the kinetics of polar nanoregions and the physical models of the relaxor ferroelectrics to illustrate the structural evolution from a relaxor to a ferroelectric state.

PACS number(s): 77.84.Dy, 61.10.−i, 77.80.−e

I. INTRODUCTION

Research on relaxor ferroelectrics and related materials has undergone an accelerated growth both in fundamental understanding of the structural and physical properties and in practical applications. The complex perovskite Pb(Mg$_{1/3}$Nb$_{2/3}$)O$_3$ (PMN) exhibits typical relaxor ferroelectric properties,[1] characterized by the frustration of local polarization due to composition and field inhomogeneities, which prevents long-range ferroelectric order from developing completely. The mechanism of the relaxor ferroelectric behavior continues to be a fascinating puzzle. Experimental data from neutron scattering,[2] nuclear magnetic resonance (NMR),[3] and measurements of nonlinear dielectric susceptibility[3,4] pointed to the existence of a nonergodic structural glassy state in relaxors below a certain temperature. It is usually believed[3,5,6] that reorientational polar species responsible for the glassy behavior are composed of the clusters of the low-symmetry structure having a size of a few nanometers, observed in relaxors. Recently, by means of dielectric spectroscopy, Bokov and Ye[7–9] have discovered a universal relaxor dispersion in PMN and related materials with different degrees of ferroelectric ordering, and showed that it is an important common property of relaxor ferroelectrics. The universal relaxor polarization is described by a microscopic model consisting of "soft" polar nanoregions (PNR's) with unit cells that can freely choose several different directions, while the direction of the total moment of the nanoregion remains the same.[9] Such an approach makes it possible to apply a standard spherical model to relaxor ferroelectrics, which predicts the experimentally observed quadratic divergence of susceptibility above the critical temperature. This model is complementary to the so-called spherical

random bond-random-field model proposed to explain the NMR data and the nonlinearity of the total dielectric susceptibility in relaxors.[3,6]

From the structural point of view, the average symmetry of PMN, when probed by conventional x-ray or neutron-diffraction techniques, appears to be cubic ($Pm\bar{3}m$) down to very low temperature with no evidence of macroscopic structural phase transition taking place through or below the temperature of maximum permittivity ($T_{\max} = 265$ K, at 1 kHz). However, diffuse scattering on the diffraction patterns were observed below the so-called Burns temperature T_d (or T_B) ≈ 600 K, indicating the presence of locally polar regions of rhombohedral $R3m$ symmetry, the volume ratio of which (over the cubic matrix) increases upon cooling to reach about 25% at 5 K.[10–13] Such an evolution of local structure is in agreement with the deviations from linearity of the refractive index,[14] the lattice parameters, and the thermal expansion and strain,[10,15] which result from the presence of PNR's. The dielectric permittivity shows a deviation from the Curie-Weiss law below T_d. A macroscopic ferroelectric phase can be induced by application of an electric field along $[111]_{\text{cub}}$, associated with cubic to rhombohedral symmetry breaking, as revealed by optical domain, dielectric, polarization, and structural studies.[16,17] Recent neutron-scattering studies have identified a ferroelectric soft mode in PMN at 1100 K that becomes overdamped near 620 K, suggesting a direct connection between the soft mode and the PNR's.[18] More interestingly, at lower temperature the soft mode in PMN reappears close to $T_C = 213$ K,[19] temperature at which the electric-field-induced polarization vanishes spontaneously upon zero-field heating,[16] and a sharp peak in the temperature dependence of the hypersonic damping appears.[20] To interpret the measured intensities of the diffuse scattering in

PMN in accordance with the concept of a ferroelectric soft mode, Hirota *et al.*[21] have proposed, and demonstrated the validity of, a phase-shifted condensed soft-mode model of the PNR's, i.e., the displacement of PNR's along their polar directions relative to the surrounding cubic matrix (*H* shift). Therefore, the phonon dynamics clearly indicates the ferroelectric nature of the relaxor PMN below T_C, although the average structure of the system remains cubic.

The substitution of Ti^{4+} for the complex $(Mg_{1/3}Nb_{2/3})^{4+}$ ions in the solid solution system between relaxor PMN and ferroelectric $PbTiO_3$ (PT), $(1-x)$PMN-xPT (PMN-xPT), results in a macroscopic ferroelectric phase with a morphotropic phase boundary (MPB) initially located at $x \approx 0.33$,[22–24] separating the rhombohedral (relaxor side of the solid solution) and tetragonal (ferroelectric side) phases. Single crystals of PMN-PT with a composition near the MPB are technologically promising materials for electromechanical transducers thanks to their excellent piezoelectric performance.[25] Intensive investigation has recently been undertaken on the structure of the MPB phases and the related properties.[26] A new MPB phase diagram of the PMN-PT system has recently been established by Noheda *et al.* based on high-resolution synchrotron x-ray-diffraction data, which reveals the presence of an intermediate monoclinic phase existing in between the rhombohedral and the tetragonal phases.[27] Therefore, a spectrum of structures and a variety of macroscopic properties can be tuned by Ti^{4+} substitution, ranging from a disordered relaxor state, to ferroelectric rhombohedral $R3m$, monoclinic Pm (M_C), and tetragonal $P4mm$ phases.

The PMN-xPT solid solutions with low concentrations of PT ($x \leq 0.15$) are also important materials for a wide range of applications, such as multilayered capacitors, electromechanical transducers, etc., especially in the form of ceramics.[28] However, different results have hitherto been reported by different groups on the structural nature of those compositions. Jang *et al.*[29] found that PMN-xPT with $x \leq 0.13$ exhibits typical relaxor ferroelectric behavior associated with a PMN-like pseudocubic structure. X-ray structural studies on $x=0.05$ and 0.10 single crystals by Bunina *et al.* seemed to confirm that result.[30] Based on neutron powder-diffraction data, Fujishiro *et al.* reported that no long-range order can develop in PMN or PMN-0.1PT at low temperature unless an electric field is applied that induces a macropolar phase.[13] Recently, Dkhil *et al.*[31] observed that in PMN the intensity of the diffuse scattering on the x-ray- and neutron-diffraction patterns appearing at about 350 K increases upon cooling and plateaus below $T_f \approx 200$ K, at which an abrupt change occurs in the slope of the variation of the lattice constant. Such an anomaly provides supplementary evidence for the ferroelectric ordering in unpoled PMN, consistent with the phonon energy recovery[19] and the hypersonic damping anomaly at $T_C = 213$ K (Ref. 20) (note that the temperature T_f identified in Ref. 31 actually corresponds to the T_C of PMN discussed above). In PMN-0.10PT, the diffuse intensity was found to increase upon cooling and shows an unusual critical divergence at $T_C = 285$ K (although the q value was not specified), associated with a structural transition into a long-range rhombohedral phase.[31] On the other hand, Koo

et al. showed that, in PMN-0.20PT, the diffuse intensity on neutron scattering at $Q=(1.04, 0, 0.96)$ peaks near $T_C \approx 380$ K, but stays up below T_C without divergence.[32]

Therefore, such fundamental questions as the nature of ferroelectric ordering in PMN and the development of PNR's into a mesoscopic or macroscopic ferroelectric state upon substitution of PT in the PMN-xPT solid solution still remain unclear. The objective of the present work is to investigate the variation of the phase symmetry in PMN-xPT ceramics ($x \leq 0.15$) as a function of temperature and composition. The structural analysis based on the experimental data from high-resolution synchrotron x-ray diffraction allows us to reveal the establishment of a rhombohedral polar phase in PMN-xPT with $x \geq 0.05$. The results are discussed in light of the kinetics of polar nanoregions and the physical models of the relaxor ferroelectrics to illustrate the structural evolution from a relaxor to a ferroelectric state.

II. EXPERIMENT

The complex perovskite samples of $(1-x)Pb(Mg_{1/3}Nb_{2/3})O_3 - xPbTiO_3$ (PMN-xPT or PMN-$100x$PT), with nominal compositions $x=0$, 0.05, 0.10, and 0.15, were prepared in the form of ceramics using an improved two-step columbite precursor method.[33] In the first step, the starting oxides of MgO and Nb_2O_5 (>99.9%) were thoroughly ground in ethanol, cold pressed into a pellet, and calcined at 1100 °C for 12 h to form the pure columbite phase of $MgNb_2O_6$ (the stoichiometry was achieved by careful weight compensation of MgO based on our thermal gravimetric analysis, since commercial MgO is well known to adsorb a significant amount of moisture and CO_2 from the atmosphere). In the second step, the columbite precursor powder was reacted with PbO or PbO and TiO_2, according to $PbO+xTiO_2+[(1-x)/3]MgNb_2O_6 \rightarrow Pb[(Mg_{1/3}Nb_{2/3})_{(1-x)}Ti_x]O_3$, with 2 wt % excess of PbO added to compensate for the evaporation of PbO during the subsequent calcining and sintering processes. Each composition was thoroughly ground and calcined at 900 °C for 4 h. The calcined powder was then reground with the addition of a few drops of binding agent [polyvinyl alcohol (PVA)] and cold pressed into a pellet of about 3-mm thick and 15-mm in diameter, which was first heated up to 650 °C in a Pt crucible for 1 h in open air to drive off the PVA, and then sintered at 1230 °C for 4 h in a sealed aluminum crucible with a PbO-enriched atmosphere to form high-density ceramics. The light yellow ceramic pellets were polished with fine diamond paste and ultrasonically cleaned. X-ray patterns obtained on a conventional diffractometer with Cu $K\alpha$ confirmed the formation of a pure perovskite phase with no evidence of any impurities.

Synchrotron x-ray powder-diffraction experiments were performed on unpoled samples at beamlines X7A (for PMN-5PT and PMN-10PT) and X3B1 (for PMN and PMN-15PT) at the Brookhaven National Synchrotron Light Source. A double-crystal channel-cut Si (111) monochromator was used in combination with a Ge (220) analyzer and a scintillating detector. The wavelength was set to $\lambda \approx 0.7$ Å and calibrated
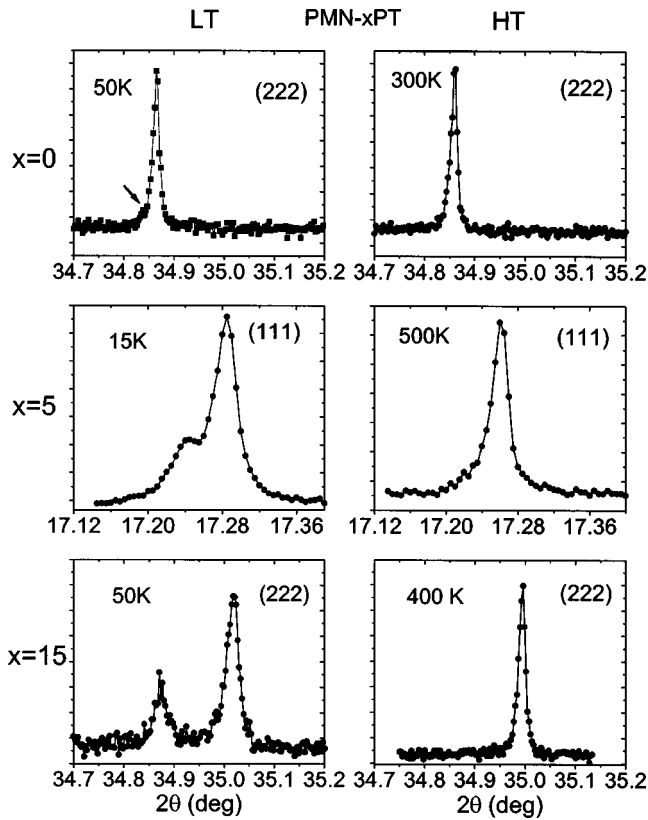
FIG. 1. Selected (222) or (111) diffraction patterns of PMN-xPT ($x = 0$, 5%, and 15%) ceramics at low and high (above T_C) temperatures.
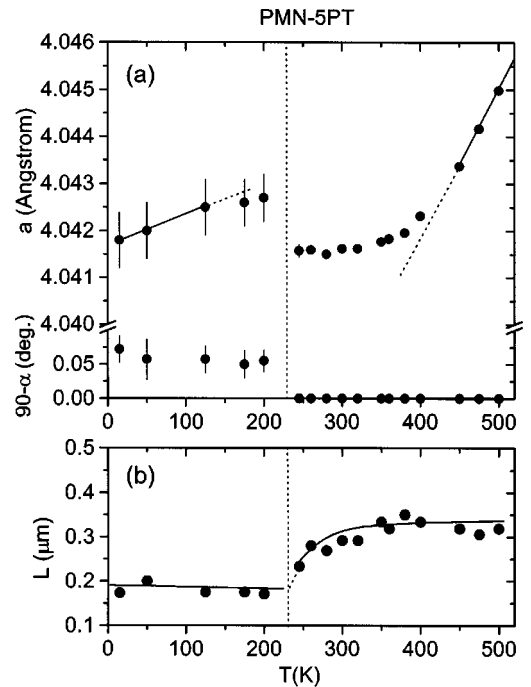

FIG. 2. Variations of (a) the cubic or rhombohedral lattice constants a and α and (b) the coherence length (L), as a function of temperature for PMN-5PT.

with a Si reference standard. The resulting instrumental resolution [full width at half maximum (FWHM)] is about 0.005° on the 2θ scale, an order-of-magnitude better than that of a conventional laboratory instrument. At X7A, the data were collected directly from the ceramic pellets loaded on a symmetric "flat-plate" reflection (Bragg-Brentano) geometry with step scans at 0.005° intervals over selected angular regions while the sample was rocking over 1°–2° to obtain better powder averaging results. The measurements as a function of temperature were performed between 20 and 500 K. For low-temperature measurements, the samples were loaded in a closed-cycle He cryostat, which has an accuracy of about ±2 K. The measurements above room temperature were carried out with the samples loaded inside a wire-wound BN tube furnace with an accuracy of ±3 K. At X3B1, the data were collected with rotating capillaries and Si powder was used as a standard at each temperature so that the accuracy in the calculated lattice parameters was within 0.0003 Å. In most of the cases, the scans were carried out over narrow angular regions centered about the six pseudocubic reflections (100), (110), (111), (200), (220), and (222), in order to determine the crystal symmetry and related lattice parameters. For data analysis, the individual reflection profiles were fitted by least squares to a pseudo-Voigt function appropriately corrected for asymmetry,[34] with intensity, peak position, and peak width (FWHM) as variables, to determine the lattice parameters.

III. RESULTS

The selected (222) or (111) diffraction patterns of PMN, PMN-5PT, and PMN-15PT at various temperatures are given in Fig. 1. Since the Curie temperature T_C increases as the composition xPT increases in PMN-xPT, the data at 300 for $x = 0$, at 500 for $x = 5$, and at 400 K for $x = 15$ were presented in Fig. 1 to make a clear comparison of the behavior of selected diffraction peaks for the high- (above T_C) and low-(below T_C) temperature phases. It can be seen that at high temperatures, all the three samples exhibit a single (222) or (111) reflection peak, in agreement with the perovskite cubic symmetry of the PMN-PT system. At 50 K, pure PMN basically shows a single (222) peak except for a weak diffuse kink that occurs at $2\theta = 34.84°$. The (111) reflection of PMN-5PT no longer remains singlet at 15 K, but splits with a shoulder that peaks at a lower angle. The (111) reflection of PMN-10PT exhibits a clear split at low temperatures with a narrow linewidth (not shown). The lower row in Fig. 1 shows the (222) reflection of PMN-15PT that clearly splits into two peaks located at $2\theta = 34.87°$ and $35.02°$ with an intensity ratio of about 1:2, as expected for a pure rhombohedral phase. The splitting of the (111) or (222) reflection in PMN-xPT ($0.05 \leq x \leq 0.15$) indicates the formation of a rhombohedral phase at low temperatures. The rhombohedral lattice parameters were calculated from (222), (200), and (220) peaks. The whole diffraction patterns were consistent with the rhombohedral symmetry, even though in most of the cases only those three peaks were followed as a function of temperature. Note that the data for PMN-5PT and PMN-10PT were measured on the ceramic pellets, and, in principle, are not free from the effects of preferred orientation and texture that affect the intensity profiles (but do not alter
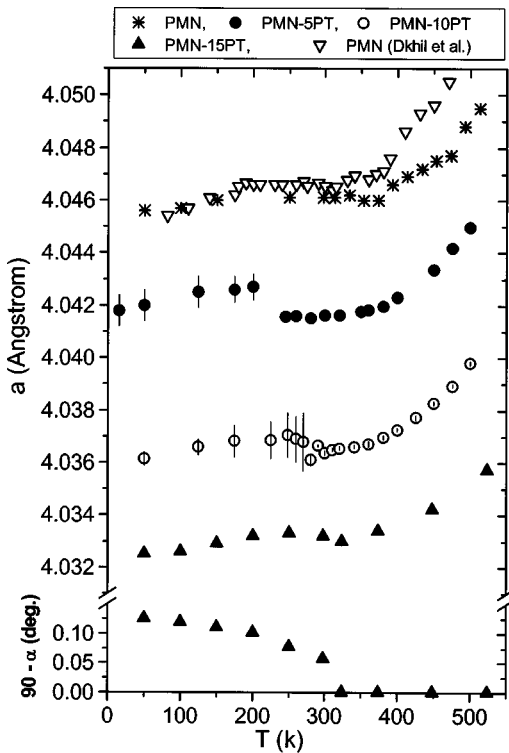
FIG. 3. Variation of the cubic and rhombohedral lattice constant *a* and the deviation of angle $(90-\alpha)$ as a function of temperature for $(1-x)$PMN-*x*PT (with $x=0$, 5%, 10%, and 15%). One of the two sets of data on pure PMN ($x=0$) was taken from Ref. 31 for comparison.

the lattice parameters so determined). That is why the intensity ratio of the (111) peaks for PMN-5PT look more like 1:3, rather than 1:2, as observed for PMN-15PT in the same figure. As can be seen from Fig. 2 (see below), the effect of the composition (x) on the lattice constants outperforms that of temperature. Therefore, the shift in the peak position arises mainly from the composition effects.

Figure 2(a) presents the variation of the cubic or rhombohedral lattice parameters, a and α, as a function of temperature for PMN-5PT. Upon cooling, the unit-cell dimension a first decreases linearly until about 430 K, then considerably curves up with a nearly zero slope between 350 and 245 K. Then, it undergoes an abrupt increase between 245 and 200 K, which is accompanied by a slight deviation from 90° of the angle α ($\Delta \alpha \approx 0.05°$), indicating the onset of the rhombohedral phase. Upon further cooling, a decreases almost linearly below 125 K while α increases slightly. In Fig. 2(b), the variation of the coherence length (L) is shown as a function of temperature. L has been extracted from the Williamson-Hall plots:[35] $\Gamma \cos \theta = \lambda/L + 2(\Delta d/d)\sin \theta$, where Γ is of the FWHM. The $\Gamma \cos \theta$ vs $\sin \theta$ relation was plotted for each temperature from the (100), (110), (111), (200), and (220) peaks, forming a set of lines. The intercept of each line in the ordinate axis was used to calculate the value of L [see Ref. 27 (Noheda *et al.*) for more details of the calculation]. The coherence length decreases upon cooling, more sharply closer to the cubic to rhombohedral phase transition, then suddenly becomes temperature independent at $T_C \approx 230$ K,
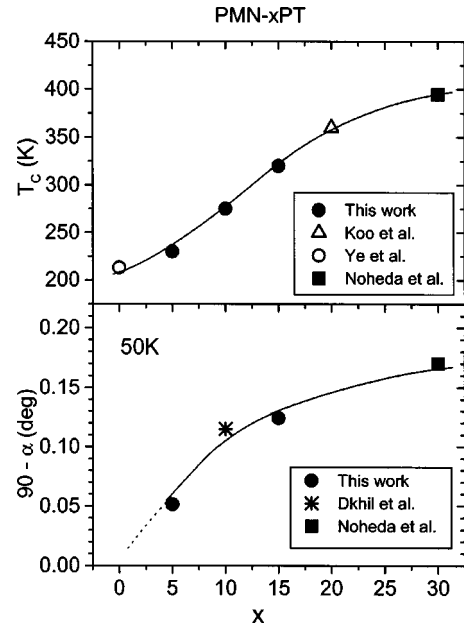

FIG. 4. Variation of the Curie temperature T_C and the rhombohedral angle α (at 50 K) as a function of composition for PMN-*x*PT. Data on PMN (T_C), PMN-10PT (α) PMN-20PT (T_C), and PMN-30PT (T_C and α) were taken from Refs. 16, 31, 32, and 27 (Noheda *et al.*), respectively, to better illustrate the trends.

and remains almost constant below T_C.

Figure 3 gives the variation of the cubic or rhombohedral lattice constant a and the deviation of angle $(90-\alpha)$ as a function of temperature for PMN and PMN-*x*PT. As in the case of PMN-5PT, the variation of the lattice constant a of PMN-10PT and PMN-15PT shows an anomaly at $T_C \approx 275$ and 320 K, respectively, where the rhombohedral distortion appears with the angle α deviating from 90°. In Fig. 3, we also plotted the cubic lattice parameter of PMN taken from Ref. 31 for comparison. Our data basically shows the same value and temperature dependence as reported in Ref. 31, except for a slight discrepancy arising in the high-temperature range ($T>400$ K), where the temperature variation of the lattice constant determined in this work exhibits a smaller slope. Figure 4 gives the variation of the Curie temperature T_C and the rhombohedral angle α (at 50 K) as a function of the composition of PMN-*x*PT. From Figs. 3 and 4, it can be seen that with increasing PT content, the following phenomena occur: (i) The lattice parameter a decreases; (ii) the cubic/rhombohedral phase transition occurs at higher temperatures, from $T_C \approx 230$ K for PMN-5PT to $T_C \approx 320$ K for PMN-15PT; (iii) the rhombohedral distortion at low temperatures enhances, with $\alpha \approx 89.95°$ for PMN-5PT, to $\alpha \approx 89.875°$ for PMN-15PT, at 50 K; and (iv) the changes of lattice parameters and unit-cell volume at the cubic/rhombohedral transition become less sharp.

IV. DISCUSSION AND CONCLUSIONS

A. Ferroelectric ordering in PMN-*x*PT

The structural analysis based on high-resolution synchrotron x-ray diffraction has allowed us to reveal some impor-

tant aspects of the structural transformation in the solid solution system of PMN-xPT. Pure PMN exhibits an average cubic symmetry without a significant split of the (hhh) peaks down to very low temperatures. The weak diffuse scattering observed at 50 K as a tail at the basis of the (222) reflection (Fig. 1) suggests, however, that local rhombohedral distortions indeed occur in PMN at low temperatures, probably with short-range order. This observation is consistent with the previous work by de Mathan *et al.*[11] in which a two-phase model, one of long-range average cubic symmetry, the other of rhombohedral polar symmetry due to atomic shifts giving rise to the local polar nanoregions, was introduced to better fit the static diffuse scattering observed in some (mainly high-angle) peaks of the x-ray- and neutron-diffraction patterns. Dkhil *et al.*[31] also confirmed that the polar order in PMN remains short ranged.

On the other hand, the softening of the transverse-optic lattice mode at the zone center in the paraelectric phase and the recovery of the overdamped soft mode below 220 K, recently observed by neutron scattering,[18,19] together with the anomaly in the hypersonic damping,[20] clearly indicate the onset of ferroelectric order in PMN. The correlation length of this ferroelectric order, i.e., the dimensions of the PNR's in which the resulting structural distortion occurs in PMN, seem to be just near the detectable limit of the x-ray- or neutron-diffraction techniques, so that only weak diffuse scattering reflecting the local polar symmetry can be observed. The substitution of Ti^{4+} for the complex B-site $(Mg_{1/3}Nb_{2/3})^{4+}$ ion is found to result in the decrease of lattice constant a [obviously due to the smaller ionic radius of $R_{Ti^{4+}} = 0.745$ as compared with $R_{Nb^{5+}} = 0.78$ and $R_{Mg^{2+}} = 0.86$ Å (Ref. 36)] and the development of a clean rhombohedral phase at a PT concentration as low as 5%. In PMN-10PT and PMN-15PT, we have also observed a very sharp and clean rhombohedral split, indicating the full establishment of the polar phase. The phase transition into the rhombohedral phase is clearly seen as the abrupt change of lattice constant a and the appearance of rhombohedral angle α (Figs. 2 and 3).

The jumps in a, α, and unit-cell volume at the transition become less pronounced with increasing x. This result suggests that the ferroelectric phase transition in PMN-PT with a low PT content is a first-order one, and it tends to be second order with increasing amounts of Ti. This behavior is consistent with the first-order nature of the phase transition from the field-induced ferroelectric state to the cubic phase observed in PMN at $T_C = 213$ K (Ref. 16) and the dielectric anomaly characteristic of second-order transition found in PMN-25PT.[37] Note that in the former case, the field-induced phase transition also tends to become second order with increasing field strength (E) and a tricritical point exists in the T-E phase diagram [Ref. 1 (Ye)].

These observations provide insight into the development of the ferroelectric phase in PMN-PT with regards to the previously reported results that the average structure of PMN-PT remains to be pseudocubic at low PT content and the rhombohedral phase is established only at a PT content higher than 13%,[29,30] even though a spontaneous rhombohe-

dral to cubic phase transition was reported in PMN-10PT around 285 °C, based on the temperature dependences of the dielectric constant[38] and the diffuse intensity and lattice parameter.[31]

In the paraelectric phase of the perovskite materials $a(T)$ dependences are usually linear, but in the high-temperature phase of PMN-PT one can observe (Fig. 3) a strong deviation from linearity. The character of this deviation is qualitatively the same for all the compositions studied. This implies that the PNR's still exist in the high-temperature phase of PMN-PT at a significant concentration. As mentioned above, the PNR's can be considered as local regions of the rhombohedral phase, which has a larger lattice dimension a. Thus, the increase in the number and size of the PNR's with decreasing temperature starting from T_d should lead to the progressive deviation of the average lattice constant from the linear trend expected in the pure paraelectric phase. In the same way, the decrease of the coherence length with decreasing temperature in the high-temperature phase [Fig. 2(b)] can be interpreted. The emergence of PNR's gives rise to the breaking of the coherency of the paraelectric phase due to the presence of the regions of a different (short-range rhombohedral) symmetry, as well as due to the internal strains introduced by these regions. At $T < T_C$, the coherence length, which is already that of the rhombohedral, but not the cubic, structure, does not change with temperature, indicating that the domain structure remains unchanged, the same as usually observed for a normal ferroelectric phase.

Thus, we have shown that the ferroelectric phase transition (i.e., abrupt change of structure and ferroelectric properties at certain temperature) is suppressed in PMN, but can be restored by the addition of a small ($\leq 5\%$) amount of $PbTiO_3$. On the other hand, the relaxor-type behavior related to the formation and evolution of PNR's remains almost unchanged at $T > T_C$ even with the addition of 15% $PbTiO_3$.

B. Compositional disorder and polar nanoregions

The above results on the structural and dynamic properties raise, first of all, the following question: why does the ferroelectric-type mode softening in PMN lead to the locally polar structural distortion, but not to the development of a long-range ferroelectric order? The general answer to this question is that the quenched compositional disorder in the Mg^{2+} and Nb^{5+} ionic arrangement prevents the development of the long-range ferroelectric order. Two approaches have been proposed that are compatible with the idea of displacive-type ferroelectric phase transition disturbed by compositional disorder: (i) quenched spatial fluctuations of the local Curie temperature leading to the formation of PNR's;[39] (ii) the breaking of the ferroelectric long-range order into PNR's by quenched random fields.[40] But the specific mechanisms of the influence of the compositional disorder on the ferroelectric phase transition is still a topic of intensive discussion.

The "quenched random-field" model[40] has been applied to relaxors based on an early idea of Imry and Ma[41] who

showed that in a ferromagnetic-type system with a continuous symmetry of the order parameter, the second-order phase transition should be destroyed by an arbitrary weak static random field conjugate to the order parameter, i.e., below the Curie temperature the system becomes broken into small-size domains (analogy of PNR's) instead of forming a long-range-ordered state as normally expected in the absence of the random field. The dimensions of the domains are determined by the interplay of the domain-wall energy and the statistics of the random field. The same arguments are believed to be approximately applicable to PMN, in spite of the facts that the phase transition here is of first order[16] and the symmetry of the order parameter (polarization) is not continuous. The disordered distribution of the heterovalent Nb^{5+} and Mg^{2+} ions on the same kind of lattice sites should provide the source of quenched random electric field.

To explain our results in the frame of this model, one may notice that the substitution of Ti^{4+} for (Mg^{2+}/Nb^{5+}) ions decreases the random fields, but it can hardly be considered as the main factor affecting the phase-transition behavior since the long-range ferroelectric order can be destroyed by an *arbitrary weak* random field. Another factor that can really cancel the effects of the random field is the transformation of the second-order phase transition into a first-order one (e.g., due to the change of composition). Such a kind of transformation should manifest itself in the appearance of the jump of the order parameter at T_C and thus in the increase of the domain-wall energy just below T_C. The equilibrium number of domain walls in the crystal should become smaller in this case, or in other words, the dimensions of domains should become larger. But we have found the opposite behavior in PMN-PT, i.e., a growth of domains with increasing x was observed along with the tendency for the phase transition to change from first to second order. Therefore, we prefer to describe our results in terms of the approach implying the formation of PNR's as a result of the disorder-related fluctuations of the local Curie temperature, rather than as a result of the random-field effects. Nevertheless, we do not necessarily deny the possible role of the quenched random field. In particular, a strong random field can probably force the dipole moment of PNR to point parallel to the field, preventing reorientation of this moment due to the thermal motions or the interactions with other PNR's.

C. Kinetics of phase transitions in relaxors

The next issue to be addressed is why the addition of a small amount of $PbTiO_3$ into the PMN relaxor results in a normal ferroelectric phase that appears under a relatively sharp phase transition. The relaxor to normal ferroelectric phase transition is often explained by the interactions between the PNR's, which are strong enough to provoke ferroelectric-type ordering of the PNR's below the phase-transition temperature. This approach implies that the relaxor to normal ferroelectric phase transition be considered as an order-disorder process, which is fundamentally different from the usual displacive-type ferroelectric phase transition related to the soft lattice mode. But such an ordering process

alone does not result in an abrupt change of the average lattice constant a, as indeed observed at T_C (Figs. 2 and 3).

To explain the relatively abrupt variation of the measured a (or the average unit-cell volume) at T_C, we assume a sharp isothermal increase of the size of existing PNR's leading to the change of the concentration of the rhombohedral phase, which has a larger a, in the heterophase mixture. Such an increase in the PNR size can be naturally derived from the model proposed by Bokov.[42] This model does not consider the interactions between PNR's as the main factor leading to ferroelectric order, even though it does not exclude the possible role of such interactions. Instead, it relates the behavior of phase transitions in disordered crystals to the transition kinetics. The approach used is analogous to the aforementioned treatment of random-field instability[41] in that the balance of the bulk and the surface energy of domains (or PNR's) is believed to determine their dimensions, but it is also different from the latter in that a first-order phase transition is considered and the random field is not regarded as the main reason for the creation of PNR's. It was shown that in the course of cooling below T_d, the formation of the PNR's takes place in two stages. At the first stage (when the temperature is high), the clusters of the short-range ferroelectric order (i.e., PNR's) begin to appear in the regions with a higher local Curie point. Each of these clusters has an equilibrium size, which can grow with decreasing temperature. The number of PNR's also increases with decreasing temperature as more nanoregions transform into the polar state. When the temperature is close to the mean Curie temperature T_C (denoted as T_{0m} in Ref. 42), the second stage begins, namely, the thermally activated formation of critical ferroelectric nuclei from some PNR's and their (isothermal) growth. This process is analogous to the formation of a new phase at a normal first-order phase transition. The growth of a nucleus is restricted by the collisions with its neighboring growing nuclei (like in the case of a normal phase transition) or with the PNR's that cannot be reoriented and merged into the growing nucleus for some reasons (such as "freezing" of PNR's due to low temperature or *strong* local random fields).

The resulting phase behavior depends on the value of a parameter ρ_c ($\propto T_C$), which determines the number of PNR's formed at the first stage. If ρ_c is large, there are few polar clusters. As a result, at the second isothermal stage, the nuclei of the ferroelectric phase can grow almost unrestrictedly, leading to macro- or mesoscopic ferroelectric domains and lattice distortions that can be detected by x-ray or neutron diffraction. This seems to be the case for PMN-PT with a significant concentration of PT, where ρ_c is comparatively larger due to a higher T_C resulting from the presence of the ferroelectrically active Ti^{4+} ion on the disordered B site [with increasing amounts of PT, the ferroelectric phase is further enhanced with T_C rising from 213 in PMN to 320 K in PMN-15PT (Fig. 4)]. Moreover, with a higher T_C, many of the existing PNR's can more easily be reoriented and merged into the growing nuclei after their collision, additionally increasing the size of final domains. The jump in the $a(T)$ dependencies (Figs. 2 and 3) should result from such a process, leading to the development of the rhombohedral symmetry in PMN-PT.

In PMN, however, ρ_c is smaller (since T_C is lower) and numerous PNR's already exist when the critical ferroelectric

nuclei begin to grow. Besides, every PNR is the obstacle to the growth of nuclei because it is thermally "frozen." As a result, the second step of the process (i.e., the isothermal growth of nuclei) is suppressed and the anomaly in the $a(T)$ dependence is absent. The final size of the "domains" at low temperatures remains compatible with the size of the PNR's initially formed at high temperatures, thus too small to be detected by x-ray or neutron diffraction but large enough to give rise to the recovery of a phonon soft mode and the anomaly in hypersonic damping.

Therefore, it is sensible to state that the difference between the nanopolar state in PMN and the rhombohedral phase in PMN-PT lies in the number and the size scale of the polar regions and their kinetics. The locally polar state in the relaxor PMN is therefore of a ferroelectric nature and the rhombohedral phase detected in PMN-xPT ($x \geqslant 0.05$) presents the natural development of the ferroelectric ordering triggered by Ti substitution.

As another key element of our conclusions, we note that ferroelectric order is established in PMN-xPT below T_C because of the divergence of the critical scattering and the ob-served rhombohedral distortion. This picture seems to conflict with the neutron-scattering observation that the strong diffuse scattering subsists below T_C in all relaxors so far examined, including PMN-20PT.[32] We are trying to resolve this issue experimentally very shortly. We also intend to investigate more extensively the $(1-x)$PMN-xPT system by a combination of structural, dielectric, and optical studies in order to provide deeper insight into such fascinating issues as (i) the microscopic mechanism underlying the development of ferroelectric ordering through enhanced polar interactions and (ii) the relationship between the ferroelectric ordering/structural transition (at T_C), the relaxor behavior, and the dynamics of the polarization regimes.

*Corresponding author. Email address: zye@sfu.ca

[1] See, for a review, L. E. Cross, Ferroelectrics **151**, 305 (1994); Z.-G. Ye, Key Eng. Mater. **155–156**, 81 (1998); A. A. Bokov, Ferroelectrics **131**, 49 (1992).

[2] S. B. Vakhrushev, B. Kvyatkovsky, A. Nabereznov, N. Okuneva, and B. Toperverg, Ferroelectrics **90**, 173 (1989).

[3] R. Blinc, J. Dolinsek, A. Gregorovic, B. Zalar, C. Filipic, Z. Kutnjak, A. Levstik, and R. Pirc, Phys. Rev. Lett. **83**, 424 (1999).

[4] E. V. Colla, E. Yu. Koroleva, N. M. Okuneva, and S. B. Vakhrushev, Phys. Rev. Lett. **74**, 1681 (1995).

[5] D. Viehland, S. J. Jang, L. E. Cross, and M. Wuttig, Phys. Rev. B **46**, 8003 (1992).

[6] R. Pirc and R. Blinc, Phys. Rev. B **60**, 13 470 (1999).

[7] A. A. Bokov and Z.-G. Ye, J. Phys.: Condens. Matter **12**, L541 (2000).

[8] A. A. Bokov and Z.-G. Ye, Phys. Rev. B **65**, 144112 (2002).

[9] A. A. Bokov and Z.-G. Ye, Phys. Rev. B **66**, 064103 (2002).

[10] P. Bonneau, P. Garnier, G. Calvarin, E. Husson, J. R. Gavarri, A. W. Heiwat, and A. Morell, J. Solid State Chem. **91**, 350 (1991).

[11] N. de Mathan, E. Husson, J. R. Gavarri, A. W. Heiwat, and A. Morell, J. Phys.: Condens. Matter **3**, 8159 (1991).

[12] Y. Uesu, H. Tazawa, K. Fijishiro, and Y. Yamada, J. Korean Phys. Soc. **29**, S703 (1996).

[13] K. Fujishiro, T. Iwase, Y. Uesu, Y. Yamada, B. Dkhil, J.-M. Kiat, S. Mori, and N. Yamamoto, J. Phys. Soc. Jpn. **69**, 2331 (2000).

[14] G. Burns and F. H. Dacol, Solid State Commun. **48**, 853 (1983).

[15] H. Arndt and G. Schmidt, Ferroelectrics **79**, 149 (1988).

[16] Z.-G. Ye and H. Schmid, Ferroelectrics **145**, 83 (1993).

[17] G. Calvarin, E. Husson, and Z.-G. Ye, Ferroelectrics **165**, 349 (1995).

[18] P. M. Gehring, S. Wakimoto, Z.-G. Ye, and G. Shirane, Phys. Rev. Lett. **87**, 277601 (2001).

[19] S. Wakimoto, C. Stock, R. J. Birgeneau, Z.-G. Ye, W. Chen, W. J. L. Buyers, P. M. Gehring, and G. Shirane, Phys. Rev. B **65**, 172105 (2002).

[20] C.-S. Tu, V. H. Schmidt, and I. G. Siny, J. Appl. Phys. **78**, 5665 (1995).

[21] K. Hirota, Z.-G. Ye, S. Wakimoto, P. Gehring, and G. Shirane, Phys. Rev. B **65**, 104105 (2002).

[22] S. W. Choi, T. R. Shrout, S. J. Jang, and A. S. Bhalla, Ferroelectrics **100**, 29 (1989).

[23] T. Shrout, Z. P. Zhang, N. Kim, and S. Markgraf, Ferroelectr. Lett. Sect. **12**, 63 (1990).

[24] O. Noblanc, P. Gaucher, and G. Calvarin, J. Appl. Phys. **79**, 4291 (1996).

[25] S.-E. Park and T. R. Shrout, J. Appl. Phys. **82**, 1804 (1997); S.-E. Park and W. Hackenberger, Curr. Opin. Solid State Mater. Sci. **6**, 11 (2002).

[26] See, for a review, L. Bellaiche, Curr. Opin. Solid State Mater. Sci. **6**, 19 (2002); B. Noheda, *ibid.* **6**, 27 (2002); Z.-G. Ye, *ibid.* **6**, 35 (2002).

[27] B. Noheda, D. E. Cox, G. Shirane, J. Gao, and Z.-G. Ye, Phys. Rev. B **66**, 054104 (2002); Z.-G. Ye, B. Noheda, M. Dong, D. Cox, and G. Shirane, *ibid.* **64**, 184114 (2001).

[28] R. E. Newnham, Q. C. Xu, S. Kumar, and L. E. Cross, Ferroelectrics **102**, 259 (1990).

[29] S. J. Jang, K. Uchino, S. Nomura, and L. E. Cross, Ferroelectrics **27**, 31 (1980).

[30] O. Bunina, I. Zakharchenko, S. Yemelyanov, P. Timonin, and V. Sakhnenko, Ferroelectrics **157**, 299 (1994).

[31] B. Dkhil, J. M. Kiat, G. Calvarin, G. Baldinozzi, S. B. Vakhrushev, and E. Suard, Phys. Rev. B **65**, 024104 (2002).

[32] T. Y. Koo, P. M. Gehring, G. Shirane, V. Kiryukhin, S.-G. Lee, and S.-W. Cheong, Phys. Rev. B **65**, 144113 (2002).

[33] S. L. Swartz and T. R. Shrout, Mater. Res. Bull. **17**, 1245 (1982).

[34] L. W. Finger, D. E. Cox, and A. P. Jephcoat, J. Appl. Crystallogr. **27**, 892 (1994).

[35] G. K. Williamson and W. H. Hall, Acta Metall. **1**, 22 (1953).

[36] R. D. Shannon, Acta Crystallogr., Sect. A: Cryst. Phys., Diffr., Theor. Gen. Crystallogr. **32**, 751 (1976).

[37] A. A. Bokov and Z.-G. Ye, Appl. Phys. Lett. **77**, 1888 (2000).

[38] O. Didault, M. Licheron, E. Husson, G. Calvarin, and A. Morell, Solid State Commun. **98**, 765 (1996).

[39] G. A. Smolensky, V. A. Bokov, V. A. Isupov, N. N. Krainik, R. E. Pasynkov, A. I. Sokolov, and N. K. Yushin, *Ferroelectrics and Related Materials* (Gordon and Breach, New York, 1984).

[40] V. Westphal, W. Kleemann, and M. D. Glinchuk, Phys. Rev. Lett. **68**, 847 (1992); W. Kleemann, Int. J. Mod. Phys. B **7**, 2469 (1993).

[41] Y. Imry and S.-K. Ma, Phys. Rev. Lett. **35**, 1399 (1975).

[42] A. A. Bokov, Fiz. Tverd. Tela (St. Petersburg) **36**, 36 (1994) [Sov. Phys. Solid State **36**, 19 (1994)].